

**An Effective Emissivity Model for Rapid Thermal Processing Using the  
Net-Radiation Method<sup>1</sup>**

Z.M. Zhang<sup>2,3</sup> and Y.H. Zhou<sup>2</sup>

---

<sup>1</sup> Paper presented at the Fourteenth Symposium on Thermophysical Properties, June 25-30, 2000, Boulder, Colorado, U.S.A.

<sup>2</sup> Department of Mechanical Engineering, University of Florida, Gainesville, FL 32611, U.S.A.

<sup>3</sup> To whom correspondence should be addressed. E-mail: [zzhang@cimar.me.ufl.edu](mailto:zzhang@cimar.me.ufl.edu).

## **ABSTRACT**

A reflective shield has been implanted in the lower chamber of some rapid thermal processing (RTP) systems so that the temperature of the silicon wafer can be accurately measured *in situ* with light-pipe radiometers. A better knowledge of the effective emissivity reduces the uncertainty in the temperature measurement. This paper describes an enclosure model based on the net-radiation method for predicting the effective emissivity of the wafer. The surfaces in the enclosure are diffusely emitting but the reflectance may include a diffuse component and a specular component. A parametric study is performed using this model to investigate the influence of the geometric arrangement, surface temperature and properties, and wavelength on the effective emissivity. The algorithm developed in this work may serve as a tool to improve radiometric temperature measurement in RTP systems.

**KEY WORDS:** effective emissivity; enclosure model; net-radiation method; radiometric temperature measurement; rapid thermal processing; RTP.

## 1. INTRODUCTION

As the packing density continues to increase and feature sizes continue to shrink in microelectronics, rapid thermal processing (RTP) has become a key technology in semiconductor device fabrication. In an RTP furnace, the wafer is individually heated by optical radiation, to temperatures as high as 1100 °C in just 10 s or so, in contrast to the 30-min typical ramp time in batch furnaces. The short ramp time prevents the ions to diffuse too far into the silicon, allowing the feature size to be minimized. Accurate determination of the wafer temperature is a challenging issue for RTP and thus has attracted the attention of many researchers [1-5]. Radiometric thermometry based on sapphire light pipe (or optical fiber) is the method of choice for *in situ* temperature monitoring. Because the radiometer output is proportional to the exitent (i.e., emitted plus reflected) radiance from the target, the emissivity and the surrounding radiation must be well characterized [5,6]. The emissivity of the wafer is a function of wavelength and temperature and can vary in a large range due to dopant type and concentration, surface roughness, coating layers, and patterning [4-10]. A reflective shield has been implanted in the lower chamber of some RTP systems to enhance the emissivity so that the temperature measurement uncertainty can be reduced [11,12]. Knowledge of the effective emissivity of the wafer is required to correlate the measured radiance temperature to the surface temperature.

Earlier, Bedford and Ma [13] performed a series of studies to calculate the local, hemispherical effective emissivity of diffuse cavities based on the zonal approximation of the integral equations, which were solved iteratively. Chu et al. [14] later extended this method to include a specularly reflecting lid. Monte Carlo methods have also been used

extensively to predict the effective emissivity of cavities [15-17]. Monte Carlo methods can incorporate complex directional radiative properties of the surface and may be used to evaluate the directional effective emissivity. Since a large number of ray bundles are required to achieve the desired accuracy, the Monte Carlo simulation often takes a large amount of computational time.

Recently, the net-radiation method was employed to study the lower chamber of the RTP furnace at the National Institute of Standards and Technology (NIST) [12,18]. The enclosure was divided into small surfaces and their radiosities were calculated by solving the matrix equation without any iteration. In the present paper, we describe a somewhat general formulation of this model which, in principle, can incorporate partially diffuse and partially specular surfaces, and demonstrate the influence of various parameters on the effective emissivity. The objective is to develop a robust and convenient tool for radiometric temperature measurement in RTP systems.

Our model is idealized based on NIST's RTP furnace [12], whose lower chamber may be regarded as a cylindrical enclosure that consists of a silicon wafer with a guard ring as the top surface, a reflective shield (over a cold plate) as the bottom surface, and a guard tube as the lateral surface (see Fig. 1). The light pipe views a small portion of the wafer through an opening (i.e., radiometer hole) at the center of the shield. The wafer is supported by three 2-mm-diameter alumina rods, which are neglected in the present model. Some additional holes on the shield are also neglected so that the model will be axisymmetric. The radius of the wafer is 100 mm and that of the shield is 135 mm. The distance between the wafer and the shield ( $L$ ) is taken as a variable with a typical value of

12.5 mm. The narrowband filter radiometer used at NIST has a central wavelength  $\lambda = 0.955 \mu\text{m}$ . The emissivity of lightly doped silicon at 800 °C is approximately  $\epsilon_w = 0.65$ .

## 2. ANALYSIS

For an enclosure consisting of  $N$  opaque surfaces, when the emitted radiation is diffuse and the reflected radiation is composed of a diffuse component and a specular component, the reflectance ( $\rho$ ) and the emissivity ( $\epsilon$ ) of each surface are related by

$$\rho = \rho^d + \rho^s = 1 - \epsilon \quad (1)$$

where superscripts  $d$  and  $s$  denote correspondingly the diffuse and specular components. It is assumed that  $\rho^d$  and  $\rho^s$  are independent of the direction but may be dependent on the wavelength. The specular view factor (also called exchange factor),  $F_{i-j}^s$ , between surface  $A_i$  and surface  $A_j$  is defined as the fraction of diffuse radiant energy leaving  $A_i$  that reaches  $A_j$  by direct travel and by a number of specular reflections [19-21]. The portion that accounts for direct travel is the regular (diffuse) view factor,  $F_{i-j}$ . The contribution of specular reflection is the view factor between each of  $A_j$ 's virtual surfaces and  $A_i$  multiplied by the corresponding specular reflectances of the surfaces that image  $A_j$ . For the simple enclosure shown in Fig. 1, if only the reflective shield contains a specular component with a uniform reflectance over the entire shield (neglecting the radiometer hole), virtual surfaces that image the wafer, guard ring, and guard tube can be created below the shield. Similarly, if the reflectance of the wafer and the guard ring is the same and includes a specular component while the guard tube and shield are diffuse, then virtual surfaces of the shield and guard tube can be created above the wafer and the guard ring.

If the temperature and the spectral radiative properties of each surface for a given enclosure are prescribed, the net-radiation method can be applied to yield the following set of equations [19,20]:

$$\sum_{j=1}^N [\delta_{ij} - \rho_{\lambda,i}^d F_{i-j}^s] J_{\lambda,j} = \varepsilon_{\lambda,i} E_{\lambda b,i}, \quad i = 1, 2, \dots, N \quad (2)$$

where  $\delta_{ij}$  is Kronecker's delta function ( $\delta_{ij} = 1$  if  $i = j$  and  $\delta_{ij} = 0$  if  $i \neq j$ ),  $E_{\lambda b}$  is the Planck blackbody distribution that is a function of wavelength and the surface temperature, and  $J_{\lambda}$  is the spectral (diffuse) radiosity that includes emitted and diffusely reflected radiation from the surface, since specular reflections are accounted for by the exchange factors. The  $N$  linear equations can be solved by matrix inversion to obtain  $J_{\lambda,i}$  ( $i = 1, 2, \dots, N$ ) for any given wavelength. Using  $H_{\lambda,i}$  for the spectral irradiation (i.e., incoming heat flux) from the enclosure to its  $i^{\text{th}}$  surface, then

$$J_{\lambda,i} = \varepsilon_{\lambda,i} E_{\lambda b,i} + \rho_{\lambda,i}^d H_{\lambda,i} \quad (3)$$

For diffuse surfaces ( $\rho^s = 0$ ), the radiosity is the sum of the emitted and reflected radiant heat fluxes leaving the surface; whereas for specular surfaces ( $\rho^d = 0$ ), the radiosity consists of only the emitted radiant heat flux. The spectral irradiation can be expressed as

$$H_{\lambda,i} = \sum_{j=1}^N J_{\lambda,j} F_{i-j}^s, \quad i = 1, 2, \dots, N \quad (4)$$

where the reciprocal relation  $A_i F_{i-j}^s = A_j F_{j-i}^s$  has been used. The net spectral radiant heat flux leaving surface  $A_i$  is

$$q_{\lambda} = \varepsilon_{\lambda,i} (E_{\lambda b,i} - H_{\lambda,i}) \quad (5)$$

The effective emissivity of a surface is defined as the ratio of the radiant energy leaving that surface by emission and reflection (both diffusely and specularly) to that of a blackbody at the same temperature. Hence,

$$\varepsilon_{\lambda eff,i} = [\varepsilon_{\lambda,i} E_{\lambda b,i} + (1 - \varepsilon_{\lambda,i}) H_{\lambda,i}] / E_{\lambda b,i} \quad (6)$$

The integration of  $q_\lambda$  yields the net radiant heat flux from any given surface. The total radiative property is the integration of the product of the corresponding spectral property and  $E_{\lambda b}$  divided by  $E_b$  (the total blackbody emissivity power given by the Stefan-Boltzmann law). If all the radiative properties are independent of the wavelength (i.e., under the gray assumption), then subscript  $\lambda$  in Eq. (2) through (6) can be eliminated. In this case, the (total) effective emissivity of the  $i^{\text{th}}$  surface becomes

$$\varepsilon_{eff,i} = [\varepsilon_i E_{b,i} + (1 - \varepsilon_i) H_i] / E_{b,i} \quad (7)$$

Furthermore, if  $\rho^s = 0$  for all surfaces,  $F_{i-j}^s \equiv F_{i-j}$  and the expressions above reduce to the corresponding equations for diffuse-gray enclosures. The analysis here is also consistent with the formulation for enclosures consisting of diffuse and specular surfaces only [21].

It is worth noting that for an enclosure of gray surfaces for which the emissivity and reflectance are not functions of the wavelength, except in some special situations,  $\varepsilon_{\lambda eff}$  is wavelength dependent and in general different from  $\varepsilon_{eff}$  because  $H_{\lambda,i}$  is a complex function of  $\lambda$  and the temperature, geometry, and properties of each surface [13].

In the present model, the first surface on the wafer is the disk with a radius equal to that of the radiometer view spot (surface 1 in Fig. 1), and the first surface on the reflective shield consists of the 2-mm-radius disk, to simulate the radiometer hole that includes the

light pipe and the sheath. The radius of the view spot on the wafer is determined by the radius of the light pipe and  $L$  (due to beam divergence) by the simple relation [12],  $1 + L/3$  [mm]. The guard ring and the rest of the wafer and shield are divided into concentric rings of approximately equal radial increment. The guard tube is not further divided (i.e., only one surface is used). The total number of surfaces on the shield is equal to the sum of the surfaces on the wafer, the guard ring, and the guard tube. The view factor between concentric rings or between concentric ring and tube can be obtained from the view factor between concentric disks using the view factor algebra [21].

Although the temperatures and radiative properties of each surface can be individually assigned, they are assumed uniform in each zone; that is, the wafer, the guard ring, the guard tube, the radiometer hole, and the rest of the shield. The temperature of the wafer is assumed 800 °C, and the temperature of the shield, radiometer hole, and guard tube are assumed to be 27 °C for most calculations. Two cases are considered as regard to the conditions of the guard ring: the first is cold ( $T_r = 27$  °C) with a low emissivity ( $\epsilon_r = 0.1$ ) and the second is hot (with the same temperature and emissivity as the wafer). The reflectance of the gold-plated reflective shield can be as high as 0.993 ( $\epsilon_s = 0.007$ ). The emissivity of the hole is assumed to be 0.925 based on the refractive index of sapphire at 0.955  $\mu\text{m}$  [22]. Sometimes it is desired not to include the radiometer hole. This is done by simply setting the emissivity of the hole to be the same as that of the shield in the computer program. It is assumed that only the top or bottom surface may include specular components. In the case when  $\rho^s$  for the wafer is not zero,  $\rho^d$  and  $\rho^s$  of the guard ring

and wafer are set to be the same. Similarly, the properties of the radiometer hole and the shield are assumed the same when the shield includes specular reflection.

The effect of the number of surfaces was tested and the calculated effective emissivity would converge to within 0.0005 if the wafer is divided by 20 surfaces. In all our calculations, the wafer is divided into 40 surfaces to produce a smooth curve, and the guard ring is divided into 12 surfaces. It takes only a few seconds on a personal computer to run one test.

### 3. RESULTS AND DISCUSSION

The spectral effective emissivity of the wafer as a function of radius for various conditions is shown in Fig. 2 at  $\lambda = 0.955 \mu\text{m}$ . The local effective emissivity away from the center is a useful concept when the light pipe views the wafer at a inclined angle or when there is another probe somewhere that has negligible effect on the value of the effective emissivity at the specified location. The temperature and emissivity of the diffuse wafer are, respectively,  $T_w = 800 \text{ }^\circ\text{C}$  and  $\epsilon_w = 0.65$ . The temperature and emissivity of the shield are, respectively,  $T_s = 27 \text{ }^\circ\text{C}$  and  $\epsilon_s = 0.007$  (i.e., the reflectance of the shield is  $\rho_s = 0.993$ ). The temperature of the guard tube is fixed at  $T_t = 27 \text{ }^\circ\text{C}$ , and the distance between the wafer and the shield is set to  $L = 12.5 \text{ mm}$ . Other parameters of the guard ring, guard tube, and the radiometer hole are varied. As seen from Fig. 2a, the conditions of the guard ring have a strong influence on the effective emissivity distribution, especially near the edge of the wafer. The effective emissivity of the wafer becomes much more uniform when the temperature and emissivity of the guard ring approach that of the wafer. The net radiant heat flux (not shown) from the wafer has similar distribution as the (total) effective

emissivity. Calculations also show that, for  $T_r = 27$  °C, increasing  $\epsilon_r$  can only reduce the effective emissivity of the wafer. The existence of the radiometric hole reduces the effective emissivity in the central region because of its high emissivity (0.925). The influence of the hole is extended to about 60° polar angle viewed from the center of the hole (i.e., 22 mm from the center of the wafer). Attention should be paid to the minimization of the radiometer hole in the design of light-pipe probe.

The effects of the guard tube emissivity is demonstrated in Fig. 2b, without considering the radiometric hole. The temperature and properties of the guard ring are assumed the same as those of the wafer. When the emissivity of the guard tube is very low ( $\epsilon_t = 0.01$ ), it acts as a refractory surface and the effective emissivity is quite uniform for all three cases. This is the most desirable situation for temperature measurements and for the control of temperature uniformity on the wafer. For the prescribed condition, the effective emissivity decreases significantly as the emissivity of the guard tube ( $\epsilon_t$ ) is increased to 0.8. The effective emissivity is the lowest with a specular shield. When the distance between the wafer and the shield is reduced, the effect of the guard tube emissivity on the effective emissivity at the center of the wafer will decrease.

Figure 3 illustrates the wavelength dependence of the effective emissivity, where all surfaces are assumed diffuse and the radiometer hole has been neglected. Assuming that the emissivity of each surface does not depend on the wavelength, the spectral effective emissivity at the center of the wafer is calculated at several different wavelengths and plotted together with the total effective emissivity calculated using the gray model. As indicated in the figure, the temperature and properties of the guard ring are assumed the same as those of the wafer, while the temperature and properties of the guard tube are

assumed the same as those of the shield. When  $T_s \ll T_w$ , the radiant energy emitted from the shield is much smaller than that from the wafer at short wavelength. The effective emissivity should be the same for all wavelengths if  $T_s$  approaches absolute zero. As  $T_s$  increases, the emission from the shield and guard tube causes the effective emissivity of the wafer to increase. Due to the nature of the Planck distribution, the effect of  $T_s$  is stronger at longer wavelengths, yielding a much greater spectral effective emissivity at  $10 \mu\text{m}$  compared with the values at  $1 \mu\text{m}$  and  $2 \mu\text{m}$ . When  $T_s = T_w$ , that is, in the case of thermal equilibrium, the effective emissivity approaches to unity regardless of the wavelength. The selecting of wavelength is an important issue for radiometric temperature measurement.

Figure 4 shows the effects of wafer emissivity and shield emissivity on the effective emissivity at the center of the wafer, without considering the radiometer hole. The wafer is assumed at  $800 \text{ }^\circ\text{C}$  and other surfaces are assumed at  $27 \text{ }^\circ\text{C}$ . The temperature of the wafer is not so important as long as it is much greater than that of the rest of the enclosure surfaces. The emissivity of the guard ring and guard tube are assumed the same (i.e.,  $\epsilon_r = \epsilon_t = 0.1$ ). It can be seen that a specular shield results in a slightly lower effective emissivity compared with a diffuse shield. If the emissivity of the shield is 0.007, the effective emissivity of the wafer is 0.9 for  $\epsilon_w = 0.3$  and 0.96 for  $\epsilon_w = 0.5$  for a specular shield. In this case, if the wafer emissivity is determined to be 0.65 with an uncertainty of 0.01 (i.e.,  $\epsilon_w = 0.65 \pm 0.01$ ), the corresponding effective emissivity for a specular shield ( $\epsilon_s = 0.007$ ) is  $0.981 \pm 0.001$ . This would substantially reduce the uncertainty in the determination of the surface temperature from the radiance temperature. The effective

emissivity would be greater if the guard ring has the same temperature and emissivity as the wafer. The radiometer hole, however, may reduce the effective emissivity.

The effect of the distance between the wafer and the shield is studied and the results are shown in Fig. 5 for diffuse wafer and diffuse shield. The emissivity of the wafer is fixed to 0.65 and the radiometer hole is included in some cases. The temperature and emissivity of the guard ring are varied. As  $L$  approached 0, the resulting effective emissivity is the same as that predicted from the two-infinite-parallel-plate model [5,18]. With the radiometer hole, the effective emissivity is nearly the same as the emissivity of bare silicon. As  $L$  increases, the effect of the radiometer hole reduces and the effective emissivity predicted with hole approached that without the hole. With a cold guard ring, the effective emissivity reduced as  $L$  further increases.

It should be noted that the irradiation is in general not diffuse except under the condition of thermal equilibrium. If the wafer is not diffuse, the effective emissivity will depend on the direction. Directional effective emissivity may be needed for light-pipe measurements. Net-radiation method is limited to predicting hemispherical effective emissivity. The Monte Carlo method can be used to calculate the directional effective emissivity and to include more complex surface properties, such as the bidirectional reflectance distribution function (BRDF) [23], with the requirement of a long computational time. A Monte Carlo model developed for the RTP chamber will be presented in a separate paper [24]. The model presented here is advantageous in terms of convenience and speed. It can be easily used for selecting light-pipe radiometers, for correlating the radiometer reading to the surface temperature, and for heat transfer analysis

in RTP systems. It may serve as a basis to validate the more complicated Monte Carlo model.

#### **4. CONCLUSIONS**

A convenient emissivity model has been built and is recommended for use as a tool for radiometric temperature measurement and heat transfer analysis in RTP systems. The temperature and properties of the guard ring have a strong influence on the local effective emissivity of the wafer, especially away from the center. If the guard tube is kept at a much lower temperature than that of the wafer, it should be covered with a highly reflective coating. The opening of the radiometer hole needs to be taken into consideration in evaluating the effective emissivity of the wafer for light-pipe thermometry. Research is under way to examine the directional effect using the Monte Carlo method and to optimize the probe angle.

#### **ACKNOWLEDGMENTS**

This work has been supported by the National Institute of Standards and Technology (grant 70-NANB-8H0011) and the National Science Foundation (grant CTS-9875441). The authors thank Drs. Dave DeWitt and Ben Tsai for valuable discussions.

## REFERENCES

1. F. Roozeboom, *J. Vac. Sci. Technol. B* **8**:1249 (1990).
2. P.J. Timans, *Mat. Sci. Semicon. Processing* **1**:169 (1998).
3. F. Roozeboom, ed., *Advances in Thermal and Integrated Processing* (Kluwer Academic Publishers, Dordrecht, 1996).
4. P.J. Timans, *Solid State Technol.* **40**:63 (1997).
5. D.P. DeWitt, F.Y. Sorrel, and J.K. Elliott, *Mat. Res. Soc. Symp. Proc.*, **470**:3 (1997).
6. Z.M. Zhang, in *Annual Review of Heat Transfer*, C.L. Tien, ed. (Begell House, New York, 2000), Vol. 11, Chap. 6.
7. P. Vandenabeele and K. Maex, *J. Appl. Phys.* **72**:5967 (1992).
8. P.Y. Wong, C.K. Hess, and I.N. Miaoulis, *Opt. Eng.* **34**:1776 (1995).
9. J.P. Hebb and K.F. Jensen, *J. Electrochem. Soc.* **143**:1142 (1996).
10. N.M. Ravindra, S. Abedrabbo, W. Chen, F.M. Tong, A.K. Nanda, and A.C. Speranza, *IEEE Trans. Semicond. Manuf.* **11**:30 (1998).
11. A. Acharya and P.J. Timans, *Mat. Res. Soc. Symp. Proc.* **525**:21 (1998).
12. B.K. Tsai and D.P. DeWitt, in *Seventh International Conference on Advanced Thermal Processing of Semiconductors – RTP '99*, Colorado Springs, pp. 125-135 (1999). C.W. Meyer, D.W. Allen, D.P. DeWitt, K.G. Kreider, F.L. Lovas, and B.K. Tsai, in *RTP '99*, pp. 136-141.
13. R.E. Bedford and C.K. Ma, *J. Opt. Soc. Am.* **64**:339 (1974), **65**:565 (1975), **66**:724 (1976).
14. Z. Chu, Y. Sun, R.E. Bedford, and C.K. Ma, *Appl. Opt.* **25**:4343 (1986).
15. A. Ono, *J. Opt. Soc. Am.* **70**:547 (1980).

16. Z. Chu, J. Dai, and B.E. Bedford, in *Temperature, Its Measurement and Control in Science and Industry* (American Institute of Physics, New York, 1992), Vol. 6, pp. 907-912.
17. V.I. Sapritsky and A.V. Prokhorov, *Metrologia* **29**:9 (1992).
18. F. Rosa, Y.H. Zhou, Z.M. Zhang, D.P. DeWitt, and B.K. Tsai, in *Advanced in Rapid Thermal Processing*, F. Roozeboom, J.C. Gelpey, M.C. Öztürk, and J. Nakos, eds. (The Electrochemical Society, Pennington, 1999), Proc. Vol. 99-10, pp. 419-426.
19. M.F. Modest, *Radiative Heat Transfer*, (McGraw-Hill, New York, 1993), Chaps. 4-7.
20. E.M. Sparrow and R.D. Cess, *Radiation Heat Transfer*, Augmented Ed. (Hemisphere Publ. Corp., Washington, 1978), Chap. 5.
21. R. Siegel and J.R. Howell, *Thermal Radiation Heat Transfer*, 3<sup>rd</sup> ed. (Hemisphere Publ. Corp., Washington, 1992), Chaps. 6-9.
22. F. Gervais, in *Handbook of Optical Constants of Solids*, E.D. Palik, ed. (Academic Press, San Diego, 1998), Vol. 2, pp. 761-776.
23. Y.J. Shen, Z.M. Zhang, B.K. Tsai, and D.P. DeWitt, to be presented at the *Fourteenth Symposium on Thermophysical Properties*, Boulder, CO, June 25-30.
24. Y.H. Zhou, Y.J. Shen, Z.M. Zhang, B.K. Tsai, and D.P. DeWitt, to be presented at the *Eighth International Conference on Advanced Thermal Processing of Semiconductors – RTP '00*, Gaithersburg, MD, Sept. 5-7, 2000.

## Figure Captions

**Fig. 1.** Schematic of the enclosure model of the lower chamber of RTP systems.

**Fig. 2.** Spectral effective emissivity (at  $\lambda = 0.955 \mu\text{m}$ ) distribution, where  $T_w = 800 \text{ }^\circ\text{C}$ ,  $T_s = T_t = 27 \text{ }^\circ\text{C}$ ,  $\epsilon_w = 0.65$ ,  $\epsilon_s = 0.007$ , and  $L = 12.5 \text{ mm}$ . (a) The effects of radiometer hole and guard ring; (b) the effect of guard tube.

**Fig. 3.** Spectral and total effective emissivities at the center versus the temperatures of the shield ( $T_s$ ) and tube ( $T_t$ ), which are assumed the same.

**Fig. 4.** The effects of wafer emissivity and shield emissivity on the spectral effective emissivity at the center of the wafer.

**Fig. 5.** Spectral effective emissivity at the center versus the distance between the wafer and the shield.

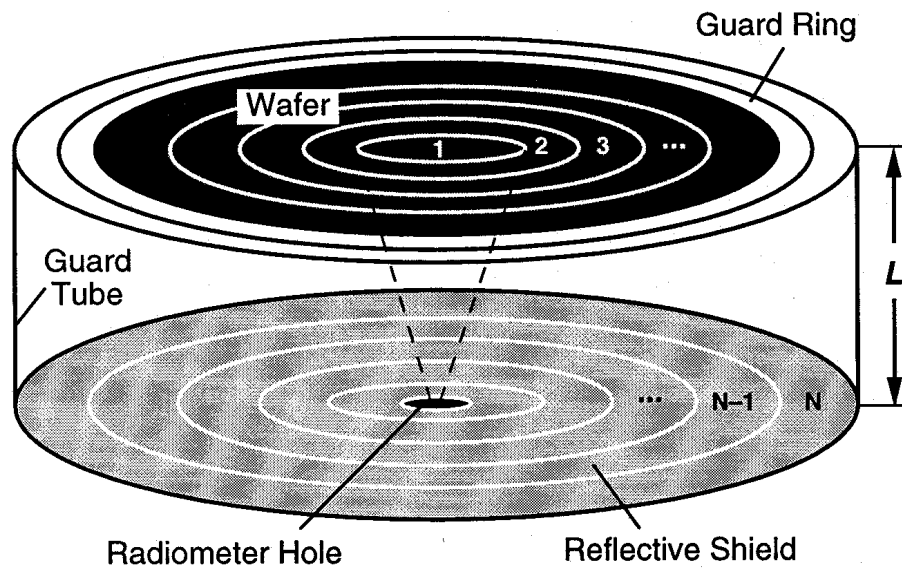


**Fig. 1.** Schematic of the enclosure model of the lower chamber of RTP systems.

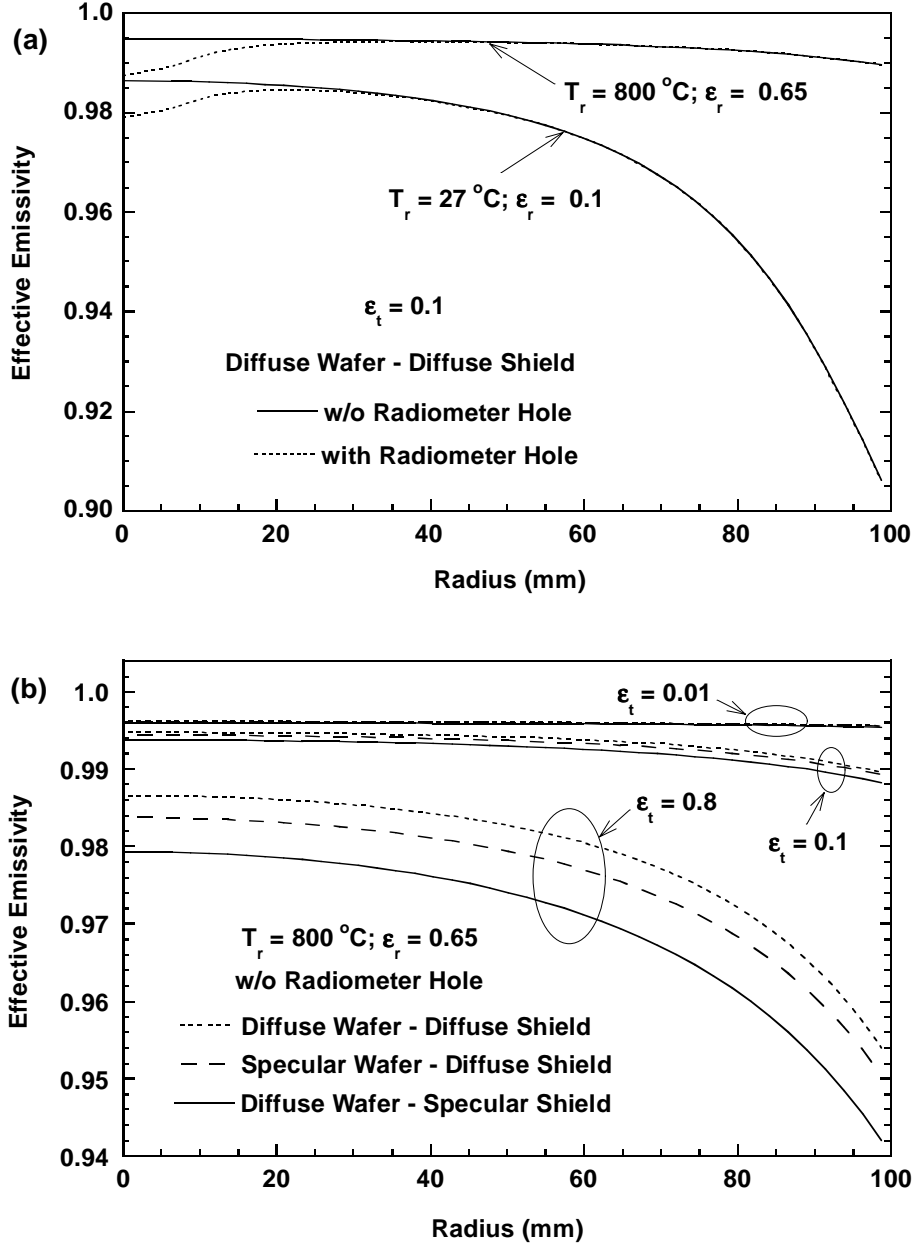


**Fig. 2.** Spectral effective emissivity (at  $\lambda = 0.955\text{ }\mu\text{m}$ ) distribution, where  $T_w = 800\text{ }^\circ\text{C}$ ,  $T_s = T_t = 27\text{ }^\circ\text{C}$ ,  $\epsilon_w = 0.65$ ,  $\epsilon_s = 0.007$ , and  $L = 12.5\text{ mm}$ . (a) The effects of radiometer hole and guard ring; (b) the effect of guard tube.

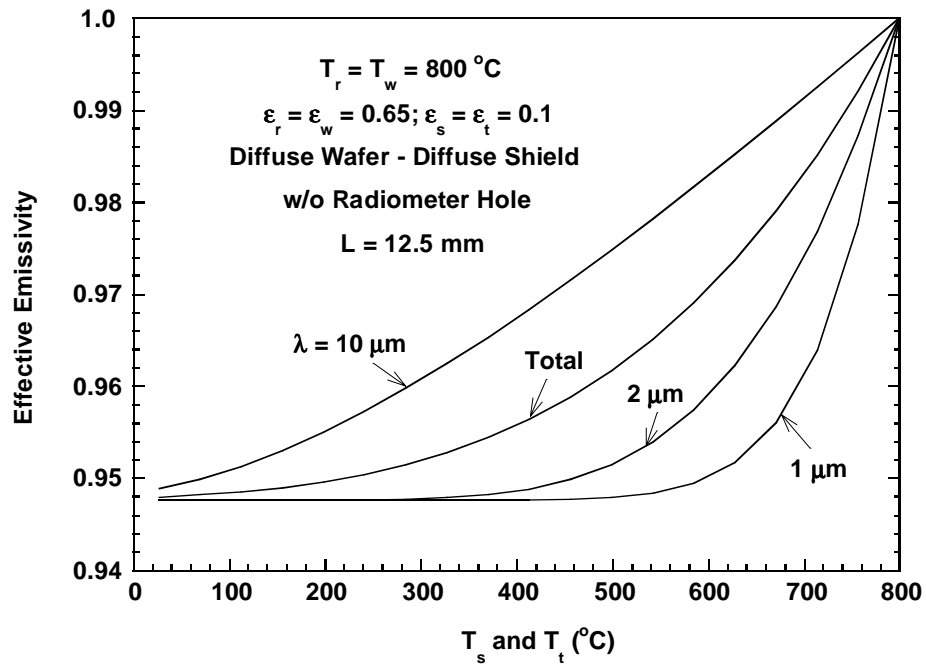


**Fig. 3.** Spectral and total effective emissivities at the center versus the temperatures of the shield ( $T_s$ ) and tube ( $T_t$ ), which are assumed the same.

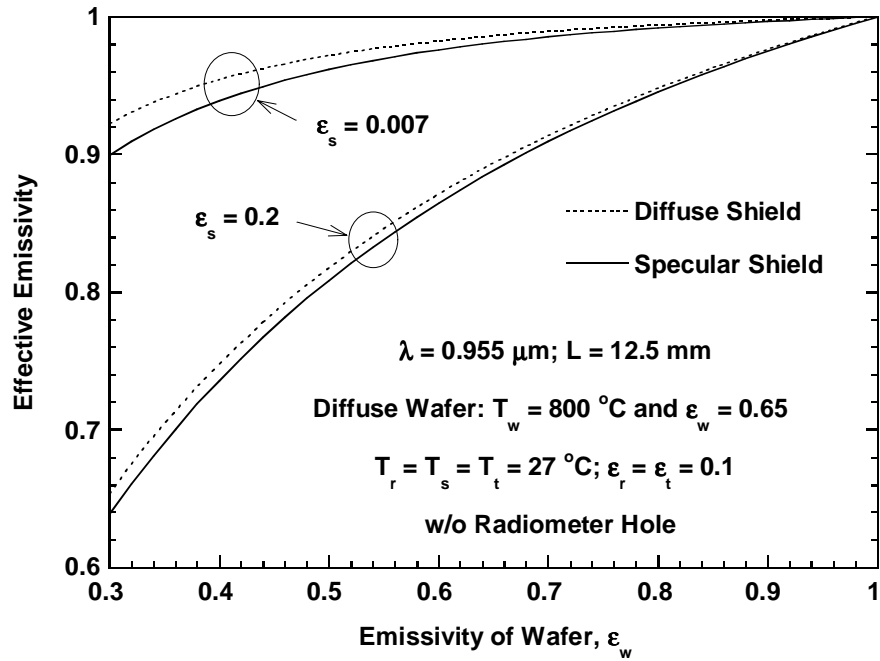


**Fig. 4.** The effects of wafer emissivity and shield emissivity on the spectral effective emissivity at the center of the wafer.

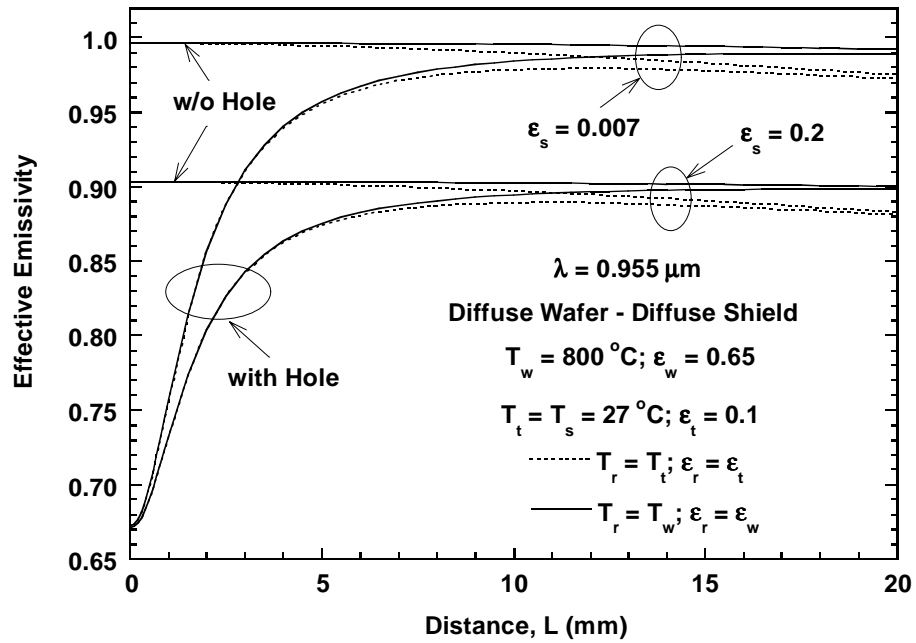


**Fig. 5.** Spectral effective emissivity at the center versus the distance between the wafer and the shield.